The Border Ranges fault system in Glacier Bay National Park, Alaska: evidence for major early Cenozoic dextral strike-slip motion

Kevin J. Smart, Terry L. Pavlis, Virginia B. Sisson, Sarah M. Roeske, and Lawrence W. Snee

Abstract: The Border Ranges fault system of southern Alaska, the fundamental break between the arc basement and the forearc accretionary complex, is the boundary between the Peninsular–Alexander–Wrangellia terrane and the Chugach terrane. The fault system separates crystalline rocks of the Alexander terrane from metamorphic rocks of the Chugach terrane in Glacier Bay National Park. Mylonitic rocks in the zone record abundant evidence for dextral strike-slip motion along north-northwest-striking subvertical surfaces. Geochronologic data together with regional correlations of Chugach terrane rocks involved in the deformation constrain this movement between latest Cretaceous and Early Eocene (~50 Ma). These findings are in agreement with studies to the northwest and southeast along the Border Ranges fault system which show dextral strike-slip motion occurring between 58 and 50 Ma. Correlations between Glacier Bay plutons and rocks of similar ages elsewhere along the Border Ranges fault system suggest that as much as 700 km of dextral motion may have been accommodated by this structure. These observations are consistent with oblique convergence of the Kula plate during early Cenozoic and forearc slivering above an ancient subduction zone following late Mesozoic accretion of the Peninsular–Alexander–Wrangellia terrane to North America.

Résumé : Le système de la faille de Border Ranges dans le sud de l'Alaska, la cassure fondamentale située entre le socle de l'arc et le complexe d'avant-arc accrétionnaire, représente la démarcation entre le terrane de Peninsular–Alexander–Wrangellia et le terrane de Chugach. Le système de cette faille sépare les roches cristallines du terrane d'Alexander d'avec les roches métamorphiques du terrane de Chugach dans le Glacier Bay National Park. Les roches mylonitiques dans la région exhibent de nombreux indices d'un mouvement de décrochement dextre, le long de plans sub-verticaux orientés nord-nord-ouest. Les données géochronologiques jointes aux corrélations régionales des roches du terrane de Chugach dérangées par les processus de déformation contraignent dans le temps ce mouvement entre la fin du Crétacé et le début de l'Éocène (~50 Ma). Ces enseignements sont en accord avec les résultats des études effectuées au nord-ouest et au sud-est, le long du système de la faille de Border Ranges, lesquels révèlent qu'un mouvement de décrochement dextre s'est produit entre 58 et 50 Ma. Les corrélations entre les plutons de Glacier Bay et les roches d'âges similaires exposées ailleurs le long du système de la faille de Border Ranges suggèrent qu'un mouvement dextre aussi important que 700 km a été accommodé par cette structure. Ces observations sont en accord avec la convergence oblique de la plaque de Kula durant le Cénozoïque précoce, et avec le morcellement de l'avant-arc au-dessus d'une ancienne zone de subduction à la suite de l'accrétion du terrane de Peninsular–Alexander–Wrangellia à l'Amérique du Nord durant le Mésozoïque tardif.
[Traduit par la rédaction]

Introduction

Studies of modern oblique convergent boundaries find that the plate-parallel motion is accommodated by trench-parallel strike-slip faults within the accretionary complex and (or) along the axis of the magmatic arc (Fitch 1972; Jarrard 1986). Many authors have suggested that the oblique convergence between the Kula and North American plates during the early Cenozoic resulted in northward displacement of terranes along the northern Cordillera (e.g., Engebretson et al. 1985, 1987; Debiche et al. 1987; Oldow et al. 1989). Determining which faults are responsible for the strike-slip displacement and timing movement has been difficult. Paleomagnetic studies indicate that the outermost terrane, the Chugach accretionary complex, was still far south of its current position with respect to North America as recently as early Cenozoic time (Plumley et al. 1983; Bol et al. 1992). In addition, the amount of early Cenozoic displacement for the Chugach terrane is greater than that for inboard terranes, indicating differential motion between the accretionary complex and its adjacent crystalline basement since the early Cenozoic (Bol et al. 1992). Our work in northern Glacier

Received August 10, 1995. Accepted April 24, 1996.

K.J. Smart[1] **and T.L. Pavlis.** Department of Geology and Geophysics, University of New Orleans, New Orleans, LA 70148, U.S.A.
V.B. Sisson. Department of Geology and Geophysics, MS-126, Rice University, Houston, TX 77005, U.S.A.
S.M. Roeske. Department of Geology, University of California at Davis, Davis, CA 95616, U.S.A.
L.W. Snee. United States Geological Survey, Denver Federal Center, MS-963, Denver, CO 80225, U.S.A.

[1] Corresponding author. Present address: Department of Geological Sciences, University of Tennessee, Knoxville, TN 37996-1410, U.S.A. (e-mail: ksmart@utk.edu).

Fig. 1. Generalized terrane map of southern Alaska showing location of Peninsular–Alexander–Wrangellia composite terrane, Chugach terrane, Prince William and Yakutat terranes, the Border Ranges fault system, and Glacier Bay National Park and Preserve (after Coney et al. 1980; Jones et al. 1981; Plafker 1987).

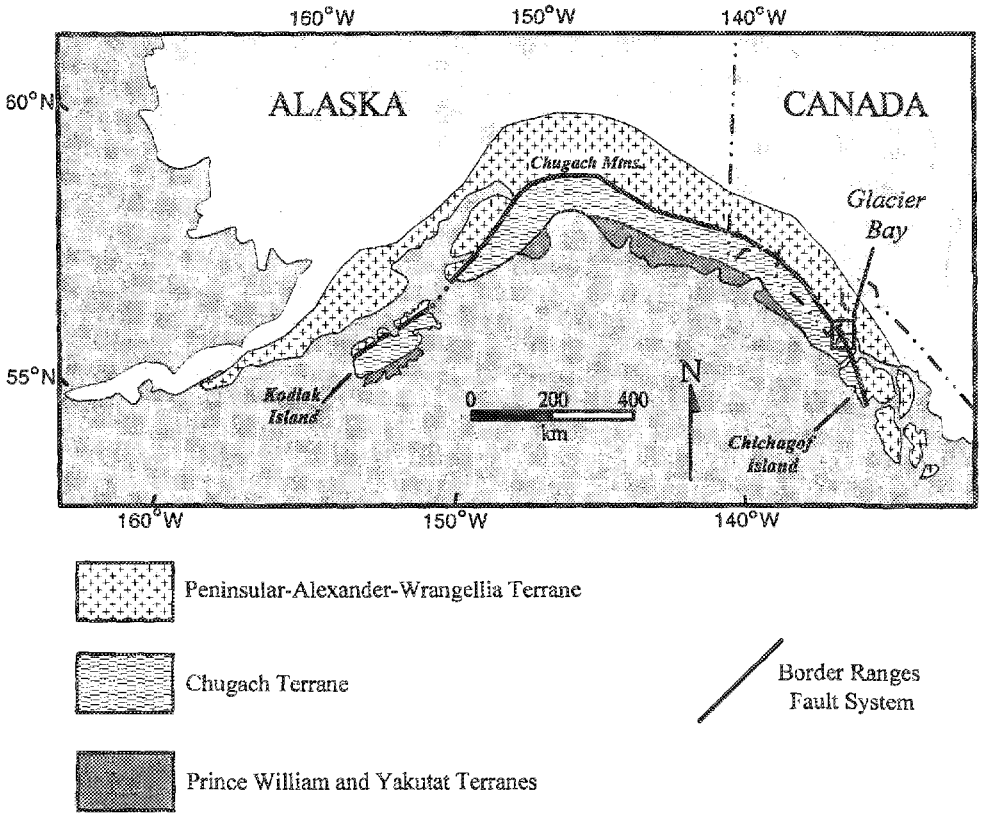

Bay, southeast Alaska, identifies a major dextral strike-slip fault system that formed at the arc–forearc boundary between the Peninsular–Alexander–Wrangellia and Chugach terranes.

Regional geology

The Border Ranges fault system (BRFS) rims southern Alaska from Kodiak Island in the west to Chichagof Island in the southeast (Fig. 1) and separates predominantly crystalline rocks of the Peninsular–Alexander–Wrangellia (PAW) terrane from the metasedimentary rocks of the Chugach terrane (MacKevett and Plafker 1974). The fault system originated as a megathrust (MacKevett and Plafker 1974; Pavlis 1982; Pavlis et al. 1988; Plafker et al. 1989, 1994), but probably moved diachronously along strike, given the great length of the fault system. Evidence for earliest motion is only locally preserved, but includes Early Jurassic subduction at the western end (Roeske et al. 1989) and Early Cretaceous reestablishment of convergence with high-temperature metamorphism and plutonism near Anchorage (Pavlis et al. 1988; Barnett et al. 1994).

Post-middle Cretaceous reactivation occurred at various times with different kinematic histories. The United States Geological Survey's Trans-Alaska Crustal Transect (TACT) program in the eastern Chugach Mountains provided the first conclusive evidence for major strike-slip reactivation, but the timing and sense of slip were unresolved (Pavlis and Crouse 1989; Plafker et al. 1989). Recent studies in the eastern Chugach Mountains (Roeske et al. 1991, 1993) clearly demonstrate a major early Cenozoic dextral reactivation. The scale of this system of brittle and ductile structures is such that it must connect to the south and east with related dextral shear systems. Nonetheless, this connection is cryptic because even reconnaissance mapping is incomplete and much of the area is under icefields of the St. Elias Range.

The BRFS emerges from ice cover and is very well exposed in the upper fiords of Glacier Bay National Park and Preserve. Reconnaissance mapping in the northernmost parts of Glacier Bay led to recognition of a 5–12 km wide, northwest–southeast-trending zone of diverse low-grade metamorphic rocks (Brew and Morrell 1978, 1979*a*, 1979*b*, 1979*c*; Brew et al. 1978*a*, 1978*b*; Decker and Plafker 1982). This zone, initially referred to as the Tarr Inlet suture zone, consists of elongate bodies of foliated diorite–granodiorite intruded into or faulted against phyllite, slate, conglomerate, chert, mélange, and marble (Brew and Morrell 1978, 1979*a*). Mélange rocks within the zone were correlated with the late Mesozoic Kelp Bay Group exposed on Chichagof Island (Decker and Plafker 1982), and by inference with other mélange units in the Chugach terrane, the Uyak Mélange of the Kodiak Islands and the McHugh Complex of the Chugach Mountains (Plafker et al. 1977). West of the Tarr Inlet suture zone is a greywacke and argillite unit that is part of the flysch subterrane of the Chugach terrane. These turbidites are prob-

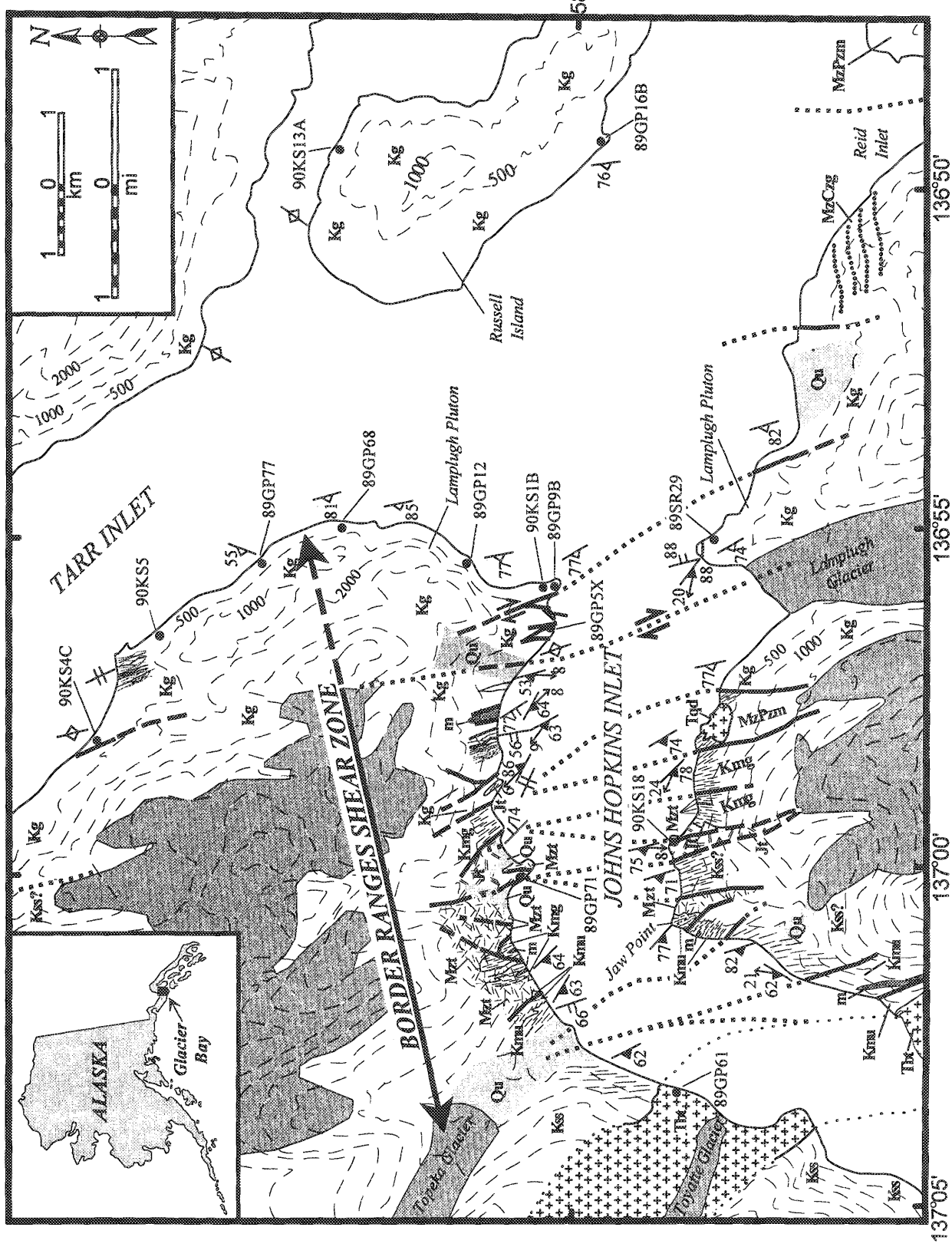

Fig. 2. Geologic map of portions of the Mount Fairweather (D-3 and D-4) quadrangles. Locations of samples used in strain analysis, geochronology, and geobarometry studies are indicated by sample number. The arrow at the end of the broken line is used for the eastern edge of the BRSZ to show that this boundary is not precisely located. The dikes west of Reid Inlet show only a generalized trend and are not meant to show precise dike locations.

Fig. 2 (*concluded*). Legend.

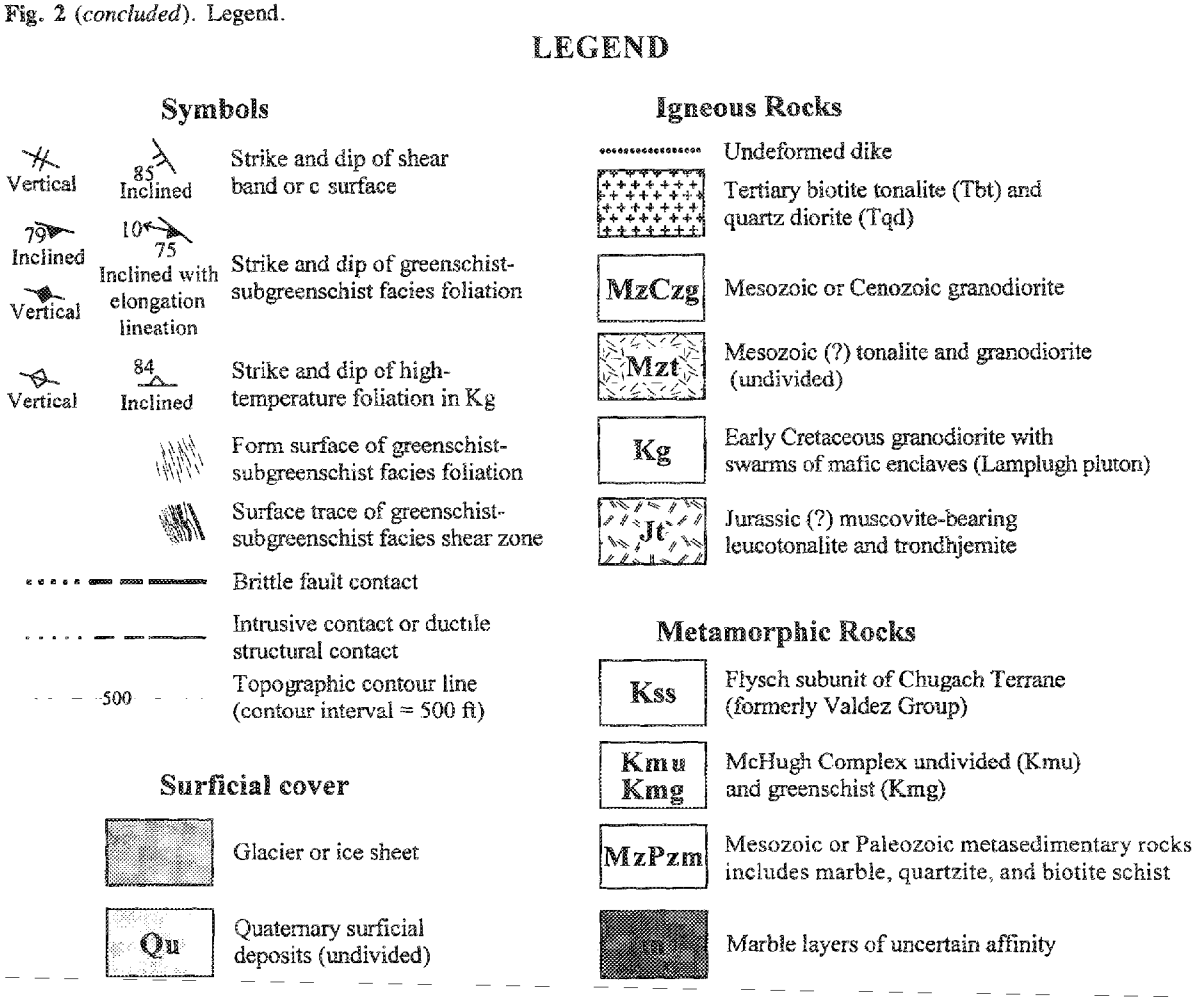

ably correlative with the Upper Cretaceous Sitka Greywacke (Brew and Morrell 1979*c*; Decker and Plafker 1982) and Valdez Group (Plafker et al. 1977).

Structural history of upper Glacier Bay

Field relations

The structural succession across the Border Ranges fault system is spectacularly exposed along the walls of Johns Hopkins Inlet (Fig. 2) in a 5–12 km wide shear zone referred to here as the Border Ranges shear zone (BRSZ). Within the BRSZ, high-angle brittle faults and ductile shear zones have complexly interleaved metasedimentary and igneous rocks of the Alexander terrane with Chugach terrane rocks (Pavlis et al. 1989; Roeske et al. 1990). East of the BRSZ, in the vicinity of Reid Inlet, Russell Island, and the eastern shore of Tarr Inlet (Fig. 2), the Alexander terrane includes a composite plutonic complex with large screens of metavolcanic and metasedimentary rocks. Here plutonic rocks are not foliated and older ductile fabrics in the metamorphic screens are overprinted by contact metamorphism.

The eastern edge of the BRSZ occurs within a large Cretaceous enclave-bearing granodiorite pluton (informally named the Lamplugh pluton). Approximately midway between Reid Inlet and Lamplugh Glacier, the first conspicuous structures related to the BRSZ appear as complex arrays of epidote veins and as discrete brittle faults (Fig. 2) showing hydrothermal alteration with pervasive epidotization and chloritization. The brittle structures are superimposed upon a high-temperature, steeply dipping fabric defined by elongate plagioclase and hornblende crystals, and aligned mafic enclaves.

Continuing westward, the first low-temperature ductile deformational structures appear as a series of retrograde ductile shear zones near the opening to Johns Hopkins Inlet. The first shear zones are relatively narrow (~10 cm to 1 m) and widely spaced but rapidly increase in thickness and abundance toward the west. The retrograde fabric is pervasive along the extreme western edge of Lamplugh pluton (~2 km west of the mouth of Johns Hopkins Inlet, Fig. 2). Extensive retrograde mineral growth in the shear zones produced a strongly foliated and lineated chlorite–epidote phyllonite from the granodiorite (Fig. 3). Foliations in the phyllonites are near vertical with subhorizontal lineations (Fig. 4*a*). Many of these shear zones are either bound by brittle faults or are cut by faults that parallel the shear bands in the phyllonites, suggesting either simultaneous brittle and ductile deformation or superposition of brittle structures onto the phyllonitic ductile shear zones.

The western limit of the Lamplugh pluton is a discrete brittle fault and to the west is a 1 km wide band of deformed greenschist showing a penetrative LS tectonite fabric with a subvertical foliation and subhorizontal stretching lineation.

Fig. 3. Outcrop photograph of ductile shear zone narrowing to brittle fault over a distance of less than a metre (pencil for scale).

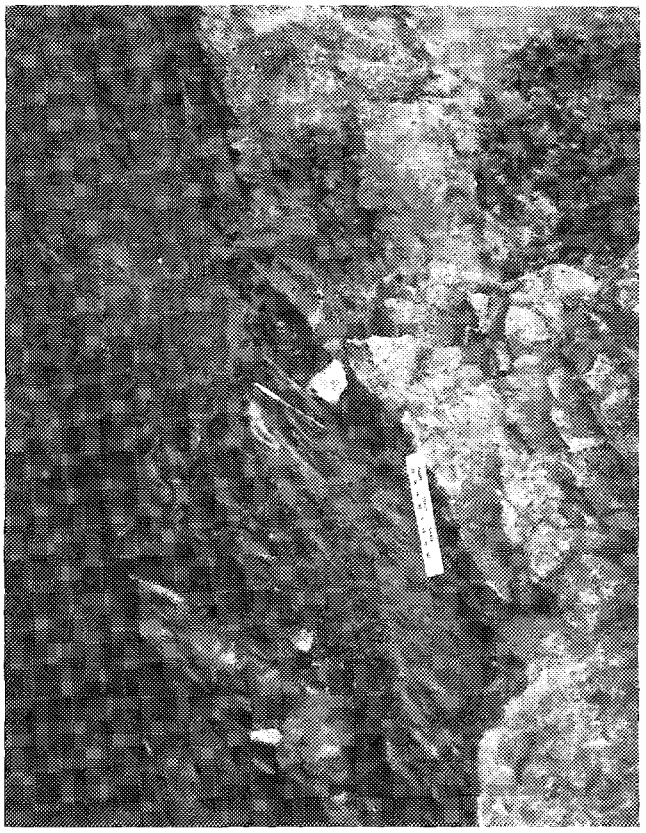

These greenschists are superficially similar to the phyllonites and could represent completely retrograded plutonic rock. Many of these rocks, however, contain thin, wispy, black, micaceous interlayers that appear to be metamorphosed argillaceous sediment. This package is probably derived from a tuff–argillite sequence, a lithology characteristic of the mélange unit of the Chugach terrane (Decker and Plafker 1982), and thus the greenschists may represent the eastern limit of that unit.

West of the greenschists, the BRSZ is a complexly juxtaposed mixture of plutonic and metasedimentary–metavolcanic rocks including greenschist, marble, and a dark meta-argillite interlayered with metagreywacke (Fig. 2). The plutonic rocks are lithologically diverse and range from hornblende diorite to muscovite trondhjemite. The metasedimentary and metavolcanic rocks presumably are derived from the diverse assemblages of the Chugach terrane, but other rocks could be present (e.g., marbles could be fragments of Alexander terrane). The phyllite–greywacke assemblage is significant because it resembles the Chugach terrane flysch to the west of the BRSZ (Fig. 2). Unfortunately, these assemblages cannot be unequivocally correlated because of a lack of fossils. Nonetheless, the phyllite–greywacke assemblages occur exclusively in the western half of the BRSZ, and slices of these rocks become more abundant westward. This structural distribution suggests that these rocks may correlate with Chugach terrane flysch. This tentative correlation is critical because the depositional age of the Chugach terrane flysch is latest Cretaceous (Plafker et al. 1994), and thus from this correlation much of the deformation in the BRSZ would be latest Cretaceous or Tertiary in age. The western edge of the BRSZ (Fig. 2) is marked by a sharp transition (i.e., fault) from highly sheared mélange to much less deformed greywacke and argillite of the flysch subterrane. The flysch is not ductilely sheared but does possess a moderately well developed, coarse, continuous cleavage subparallel to bedding. If the phyllite–greywacke assemblages within the BRSZ are correlative with the flysch to the west, then the western boundary of the BRSZ appears to be a brittle fault that postdates the main phase of shear.

Fabric development within the western half of the BRSZ is variable, but indicates a kinematic history indistinguishable from the eastern half. Brittle faults are near vertical with subhorizontal slickenlines (Fig. 4*b*) and bound heterogeneously deformed packages. Plutonic rocks typically lack a penetrative foliation, but are locally intensely deformed by systems of ductile shear zones, brittle faults, or both. Hydrothermal alteration of the plutonic rocks to chlorite–epidote assemblages is ubiquitous in both the brittle faults and the ductile shear zones. In contrast, most metasedimentary and metavolcanic assemblages display a penetrative prograde fabric. Mafic metavolcanic rocks are characterized by a greenschist facies assemblage of quartz + chlorite + actinolite + muscovite + epidote.

Structural analysis

The kinematics of the BRSZ are clearly indicated by minor structures in both the ductilely and brittlely deformed rocks. Mylonitic shear zones in quartz-rich rocks and chloritic phyllonites all have an L–S-tectonite fabric characterized by a northwest-striking, vertical to steeply west-dipping foliation with subhorizontal mineral lineations (Fig. 4*a*). Extension lineations calculated from S and C intersections, like the mineral lineations, are nearly subhorizontal (Fig. 4*a*). Fabric asymmetries, such as asymmetric pressure shadows (Fig. 5), S–C relationships, and mesoscale asymmetric porphyroclasts (Fig. 6) show clear evidence of dextral shear.

A system of brittle faults with subhorizontal slickenlines (Fig. 4*b*) is subparallel to the c surfaces and late shear zones and has dextral slip sense indicators. Thus, the low-temperature ductile and brittle deformational history was dominated by right-lateral motion. Finally, the low-temperature fabrics in the BRSZ are nearly parallel to the high-temperature foliation in the Cretaceous granodiorite along the eastern boundary (Fig. 4*c*) (see below).

Multiple dike generations

At least four generations of dikes help constrain the relative timing of deformation in upper Glacier Bay. Unfortunately, the absolute ages of the dikes are unknown. The oldest dikes postdate the Late Cretaceous plutonic complex, but predate the low-temperature ductile deformation of the BRSZ. These include garnet–muscovite trondhjemite dikes and younger mafic dikes that crosscut the high-temperature fabric in the plutonic rocks but are cut by the retrograde shear zones. The younger two generations are mafic dikes that provide important crosscutting relationships with structures of the BRSZ.

The earliest of these mafic dikes occurs predominantly as an east-southeast-striking, near-vertical swarm 4–5 km east

Fig. 4. (*a*) Equal-area, lower hemisphere projection of poles to 64 mylonitic foliation planes, showing mineral lineations (●), extension lineations calculated from S–C intersections (×), and poles to c surfaces (▲). (*b*) Equal-area, lower hemisphere projection of poles to 64 fault planes. ◆, 21 slickenline measurements. (*c*) Equal-area, lower hemisphere projection of 42 poles to high-temperature foliation planes. (*d*) Equal-area, lower hemisphere projection of poles to mafic dikes that crosscut the retrograde shear zones. □, older dikes, ■, younger dikes. All contouring uses the Kamb (1959) method with a contour interval of 3σ. Counting circle is 12.3% for (*a*) and (*b*) and 17.6% for (*c*).

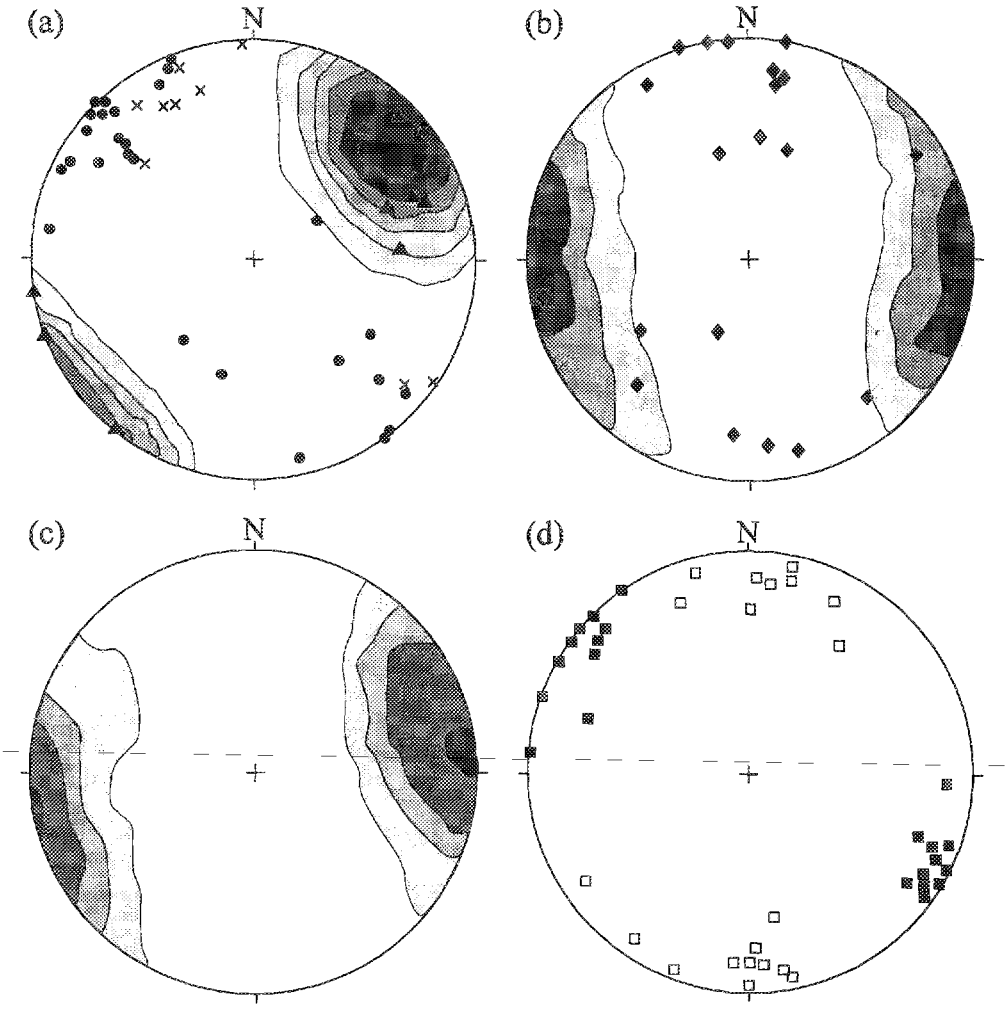

of the main BRSZ (Fig. 4*d*). These dikes are limited spatially to a single granodiorite body just west of Reid Inlet (Fig. 2), but this swarm accommodated a large north–south extension because dikes constitute more than 50% of the rock. Although the absolute age of these dikes is problematic, they are clearly cut by brittle faults related to the BRSZ. Nonetheless, because of their spatial distribution it is unclear whether these dikes are equivalent to deformed dikes within the BRSZ, or whether the injection of this complex was related to the deformation of the BRSZ.

In contrast, the youngest dikes crosscut all ductile structures, strike north-northeast, are nearly vertical (Fig. 4*d*), and have a vesicular texture with conspicuous chill margins, suggesting that this set was emplaced at a shallow level and significantly postdates major ductile deformation. Isotopic ages are lacking, but they may correlate with the Late Oligocene – Miocene mafic dike swarm in southeast Alaska and British Columbia described by Brew (1994).

Deformation of plutonic rocks along the Border Ranges shear zone

The Lamplugh pluton contains a locally well-developed high-temperature fabric subparallel to its highly elongate northwest trend and to retrograde brittle–ductile fabrics within the BRSZ. Parallelism of magmatic and tectonic fabrics may occur in oblique convergent margins, as modern examples typically have strike-slip faults parallel to and within the axis of the magmatic arc (Fitch 1972; Jarrard 1986). To test whether both the high-temperature fabric and the retrograde shear zones formed during the same progressive deformation, we assessed the finite strain state in the foliated plutonic rocks directly east of the BRSZ using the shape fabric of mafic enclaves and dimensionally preferred orientation of

Fig. 5. Thin-section photomicrograph of asymmetric pressure shadow around quartz grain indicating a dextral shear sense. Field of view is approximately 1.2 mm × 0.8 mm.

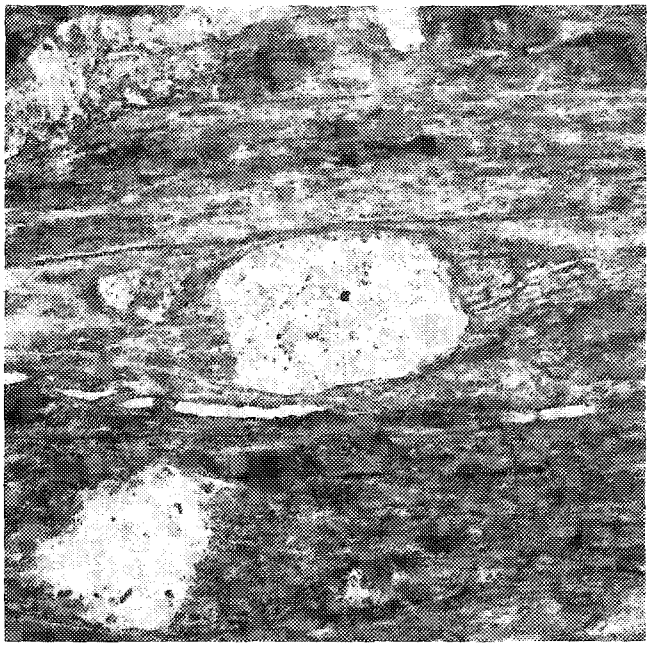

Fig. 6. Outcrop photograph of asymmetric porphyroclast showing dextral sense of motion (hammer point for scale).

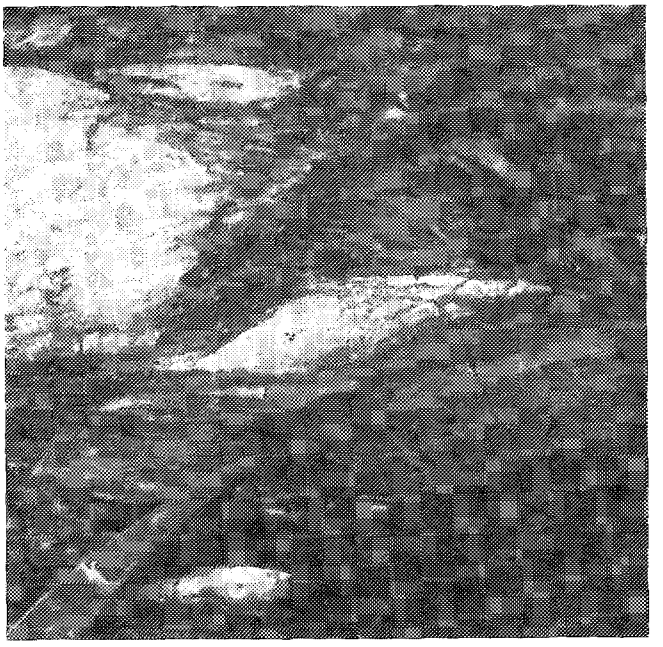

mineral grains at the thin-section scale (Ramsay and Huber 1983; Hutton 1988; Brun et al. 1990). Pitfalls for using these object strains as an accurate measure of the finite strain are that it is difficult to distinguish plutonic from solid-state fabrics (Hutton 1988; Paterson et al. 1989) and the initial shapes of the enclaves are unknown. Nonetheless, these analyses provide an approximation of the strain state.

Finite strain from mafic enclaves

The shape fabric for deformed enclaves was estimated by field measurement of ellipticities on three or more surfaces at three locations near the eastern boundary of the BRSZ (samples 89GP12, 89GP68, and 89GP77; Fig. 2). Two-dimensional shapes were estimated on each surface from the harmonic mean of 20–50 measurements of enclave ellipticity, and the finite strain ellipsoid calculated (Table 1) (Owens 1984).

The flattening (x,y) planes are subparallel to the observed field foliations (Table 1; Fig. 4*c*), although the great variation in finite strain ellipsoid shape (Fig. 7) may indicate that the deformation is apparent for a fabric that actually formed by magmatic emplacement. Alternatively, the ellipsoid shape may be a function of the interaction between emplacement and subsequent tectonic deformation. For example, the prolate strain ellipsoid (sample 89GP68; Figs. 2, 7) may indicate that locally the enclaves are extremely attenuated mafic dikes. This interpretation is supported by a field observation of a mafic dike that was traced laterally from a coherent intrusive body into boudinaged segments that resembled typical enclaves.

Thin-section-scale object strains

Finite strain was estimated in three perpendicular thin sections for six samples (Table 2) of the Lamplugh pluton using the line-strain (Panozzo 1983, 1984) and normalized Fry methods (Erslev 1988). Digitized plagioclase and quartz grain boundaries were interpreted using computer programs developed by W.A. Yonkee (written communication, 1989), and two-dimensional strain data were combined to yield finite strain ellipsoids (Owens 1984).

Most samples (Fig. 7; Table 2) fall within the field of apparent flattening. The x,y-planes strike north-northwest, and most dip moderately to steeply southwest, consistent with the observed foliations (Fig. 4*c*). The long (x) axes are generally either subhorizontal or subvertical. The bimodal variation in x-axis plunge could be an artifact of the extreme oblateness of the strain ellipsoids, in that for a strongly oblate shape, the difference between the long and intermediate axis magnitudes is small.

Origin of foliation and interpretation of strain data

The fabric observed within the Lamplugh pluton is interpreted to result from superposition of a solid-state tectonic deformation on a preexisting magmatic fabric. Evidence for the initial magmatic component includes (*i*) foliation partially defined by aligned euhedral plagioclase lathes with rare oscillatory zoning and twins parallel to the long dimension of the grains (Hutton 1988; Paterson et al. 1989; Miller and Paterson 1992), and (*ii*) aligned mafic enclaves (Hutton 1988; Paterson et al. 1989; Miller and Paterson 1992). A superimposed high-temperature solid-state component of deformation is suggested by the presence of medium- to fine-grained recrystallized hornblende and biotite adjacent to partially recrystallized plagioclase lathes (Paterson et al. 1989; Miller and Paterson 1992). Evidence for subsequent low-temperature solid-state deformation includes (*i*) moderately to strongly undulose quartz, (*ii*) chevron-style kinks in partially recrystallized biotite, and (*iii*) microfractured hornblende (Paterson et al. 1989; Miller and Paterson 1992).

In contrast to the fabrics within the plutonic rocks, the duc-

Table 1. Summary of finite strain data determined from mafic enclaves.

Sample No.	Principal planes			Axial ratios		Field foliation
	x,y	y,z	x,z	R_{xy}	R_{yz}	
89GP12	351°/84°W	089°/40°N	076°/51°S	2.47	4.12	347°/77°W
89GP68	349°/84°E	073°/45°N	084°/45°S	7.43	2.23	344°/81°W
89GP77	005°/41°W	242°/88°S	000°/48°E	2.33	2.42	020°/55°W

Notes: The principal planes and axial ratios of calculated finite strain ellipsoids are given for each sample (locations given in Fig. 2). The field foliation is given for comparison with the calculated flattening (i.e., x,y) planes.

Table 2. Summary of finite strain data determined from Cretaceous granodiorite.

Sample No.	Principal planes (line strain)			Line strain		Principal planes (Fry)			Fry		Field foliation
	x,y	y,z	x,z	R_{xy}	R_{yz}	x,y	y,z	x,z	R_{xy}	R_{yz}	
90KS1B	341°/82°S	072°/79°N	036°/14°S	1.22	1.35	341°/89°S	057°/05°S	071°/85°N	1.24	1.34	005°/90°
90KS4C	342°/80°N	072°/87°N	326°/11°S	1.04	1.51	348°/86°S	081°/48°N	073°/42°S	1.44	1.71	350°/90°
90KS13A	346°/70°W	359°/21°E	077°/86°N	1.12	1.23	325°/89°W	058°/29°N	054°/61°S	1.38	1.43	na
89GP16B	347°/57°W	008°/35°E	084°/80°N	1.17	1.53	334°/62°W	010°/34°E	084°/74°N	2.24	1.66	354°/76°W
89GP5X	327°/46°W	025°/61°E	274°/58°N	1.19	1.48	309°/48°S	080°/53°N	012°/63°E	1.39	1.79	000°/69°W
89GP9B	006°/55°W	271°/83°S	351°/36°E	1.22	1.18	012°/57°W	088°/70°S	331°/39°N	1.90	1.48	335°/77°S

Notes: The principal planes and axial ratios of finite strain ellipsoids are given for each sample as calculated by line-strain and normalized Fry methods (locations given in Fig. 2). The field foliations (where measured) are given for comparison with the calculated flattening planes. na, foliation too faint to be measured in the field.

tile shear zones formed at subgreenschist to low-greenschist facies conditions. Retrograde assemblages in the granodiorite include muscovite + chlorite + quartz ± epidote ± calcite ± albite. Quartz has undulose extinction and subgrain development, whereas hornblende and plagioclase fractured brittlely. Chlorite and muscovite also grew as fine-grained fillings between porphyroclasts of quartz and feldspar and as pressure shadows around quartz.

The strain studies support the field observation that the x,y-plane is parallel to the foliation in the rock, but elongation is poorly defined. Calculated ellipsoid long axes are scattered throughout the foliation plane and are neither consistently steeply plunging nor subhorizontal, as would be predicted by a syntectonic pluton emplaced into either a thrust or strike-slip system. The results of the strain study do not directly support the hypothesis that the high-temperature fabric and the BRSZ are the product of a single progressive deformation. However, the high-temperature fabrics are shifted 20–30° with respect to the low-temperature fabrics. Assuming progressive simple shear, the high-temperature fabric would record larger strains than the low-temperature fabric and the systematic misalignment between orientations would be produced; thus, a single progressive deformation event is possible.

The origin of the strong fabric within the plutonic body is problematic and several possibilities exist. One possibility is a fabric entirely related to emplacement (e.g., ballooning plutons as cited in Castro 1987; Ramsay 1989; or Paterson and Fowler 1993). We consider this mechanism unlikely, however, given the highly elongate shape of the pluton (Brew et al. 1978*a*; Gehrels and Berg 1994) and the clear evidence for significant solid-state deformation. Alternatively, the

Fig. 7. Flinn plot of finite strain ratios determined from mafic enclaves (■) and Cretaceous granodiorite (▲, line-strain method; ●, normalized Fry method).

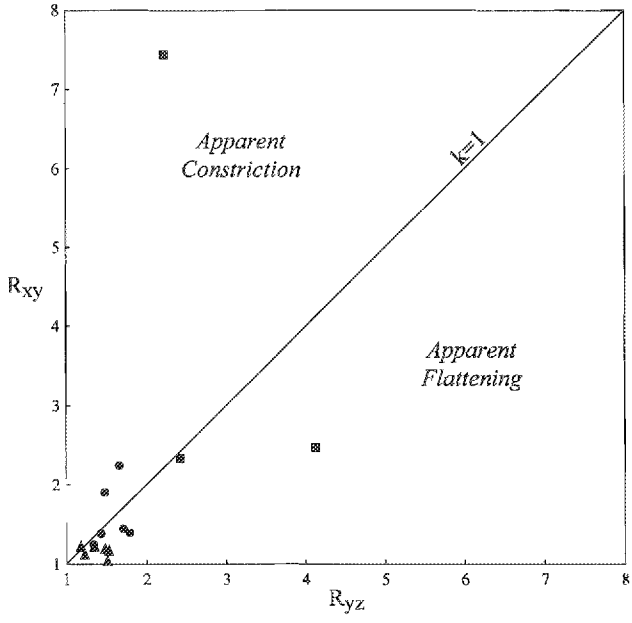

fabric could be due to a magmatic fabric with superimposed tectonic solid-state flow. A final possibility is that the pluton represents syntectonic emplacement in a zone of distributed transpression. Given that theoretical models (e.g., Sanderson and Marchini 1984; Fossen and Tikoff 1993) indicate that bulk flattening strains are required in a system subjected to

Table 3. Summary of U–Pb isotopic data for zircon from sample 89SR29 (location given in Fig. 2).

				Measured ratios			Atomic ratios			Apparent age (Ma)[a]		
Sample size (mesh units)	Weight (mg)	U (ppm)	$^{206}Pb^*$ (ppm)	$\frac{^{206}Pb}{^{204}Pb}$	$\frac{^{207}Pb}{^{206}Pb}$	$\frac{^{208}Pb}{^{206}Pb}$	$\frac{^{206}Pb^*}{^{238}U}$	$\frac{^{207}Pb^*}{^{235}U}$	$\frac{^{207}Pb^*}{^{206}Pb^*}$	$\frac{^{206}Pb^*}{^{238}U}$	$\frac{^{207}Pb^*}{^{235}U}$	$\frac{^{207}Pb^*}{^{206}Pb^*}$
100+	2.1	374	6.134	1929	0.05678	0.09608	0.01911	0.12874	0.04886	122.0	123.0	141 ± 10^b
100–206	2.3	337	5.462	1246	0.06039	0.10437	0.01884	0.12623	0.04859	120.3	120.7	128 ± 5^b

Notes: Analyses performed by J. Wright at Rice University, Houston, Texas. Pb* denotes radiogenic Pb, corrected for common Pb using the isotopic composition of $^{206}Pb/^{204}Pb = 18.6$ and $^{207}Pb/^{204}Pb = 15.6$.

[a]Ages calculated using the following constants: decay constant for $^{235}U = 9.8485 \times 10^{-10}$, $^{238}U = 1.55125 \times 10^{-10}$, and $^{238}U/^{235}U = 137.88$. Replicate analyses of "standard" zircon fractions yield reproducibility of $^{206}Pb^*/^{238}U$ of 0.05 at 2σ.

[b]The 2σ uncertainties in the $^{207}Pb^*/^{206}Pb^*$ ages were calculated on the combined uncertainties in mass spectrometry (principally the uncertainty in the $^{206}Pb/^{204}Pb$ measured ratios) and an assumed uncertainty of ± 0.1 in the $^{207}Pb/^{204}Pb$ ratio used for the common Pb correction.

distributed transpressional motions, this process could explain both the elongate shape of the pluton and the observed flattening. As a result, we favor the latter interpretation.

Timing of deformation events from geochronological studies

Isotopic dating of the dextral ductile shear zones has proven difficult because the rocks are heterogeneously deformed and the $^{40}Ar/^{39}Ar$ isotopic system has not completely reset (Roeske et al. 1992). A conservative interpretation of crystallization and cooling ages of some plutonic bodies in the BRSZ brackets the age of deformation between Early Cretaceous and Early Oligocene. However, as described below, we suggest that the deformation actually occurred primarily, if not entirely, in the early Cenozoic.

The clearest maximum age for the BRSZ is provided by U–Pb zircon and hornblende $^{40}Ar/^{39}Ar$ dates from the deformed granodiorite (i.e., Lamplugh pluton) on the eastern edge of the BRSZ (sample 89SR29, Fig. 2). The U–Pb zircon data show a slight discordance from the coarse to fine fractions (Table 3). However, the younger U–Pb ages (~120 Ma) are younger than the very clean (123.3 ± 0.4 Ma) $^{40}Ar/^{39}Ar$ hornblende plateau age (Fig. 8) (Roeske et al. 1992) for the same sample. We interpret the igneous age of the pluton to be ~130 Ma.

A significantly younger maximum age is suggested by correlation of metaclastic units within the BRSZ. Based on our experience in other parts of the Chugach terrane, the large slices of metagreywacke and argillite within the BRSZ (labeled Kss? in Fig. 2) are indistinguishable from the latest Cretaceous flysch units of the Chugach terrane (Valdez Group and Sitka Greywacke). Lithologic correlations are always ambiguous, but based on other data (discussed below) this correlation is allowable. Thus, we suggest their latest Cretaceous age is a reasonable maximum age for the deformation in the zone.

Minimum age estimates for the low-temperature deformation in the BRSZ are provided by crosscutting plutons and cooling ages. An absolute minimum age for the brittle faulting and low-temperature shear zones is provided by the large pluton in upper Johns Hopkins Inlet (sample 89GP61, Fig. 2). It cuts both fabrics and the brittle fault along the western edge of the BRSZ and yielded an $^{40}Ar/^{39}Ar$ total gas age on biotite of 33.1 ± 0.3 Ma (Table 4; Fig. 8). A potentially more useful crosscutting relation is a small undeformed diorite plug immediately west of Lamplugh Glacier in the heart of the BRSZ (Fig. 2). This undeformed pluton, however, crosscuts only ductile structures and, as such, cannot be used to constrain the cessation of brittle faulting. Decker and Plafker (1982) reported a hornblende K–Ar date of 58.6 ± 5.2 Ma for this pluton. We attempted to date this pluton to determine the reliability of this standard K–Ar date. However, thin sections revealed that the amphiboles generally contain pyroxene cores and we were unable to obtain a pure separate. This pluton is compositionally uniform, and thus we believe the separate from the original date probably contained these impurities. Pyroxene is a potential site for extraneous ^{40}Ar (e.g., McDougall and Harrison 1988); thus, we suspect that this apparent age of ~59 Ma may be too old. As a result, we submit that the only unequivocal age window for the deformation is ~130 to ~33 Ma.

To further constrain the age of the deformation, we analyzed a pair of samples from the large muscovite–leucotonalite body in Johns Hopkins Inlet (Fig. 2). The first sample (89GP71) was a coarse-grained intrusive rock with abundant coarse igneous muscovite. Because of the relatively low closure temperature for muscovite, we assumed this separate would yield a cooling age, indicating a minimum age for the deformational event. However, the plateau age of 162.1 ± 0.4 Ma (Table 4; Fig. 8) (Roeske et al. 1992) is substantially older than the maximum age for the retrograde shear zones, as indicated by the hornblende cooling age of 123 Ma (sample 89SR29). Thus, the argon isotopic system in the igneous muscovite was not reset during the low-temperature deformation in the BRSZ. Another sample (90KS18), from a 2–10 mm thick, mylonitic shear zone, contained finer grained (100–200 mesh) white mica. The result (Table 4; Fig. 8) is a classic disturbed Ar release spectrum with apparent ages gradually climbing from ~51 Ma in low-temperature steps to ages approaching the coarse-fraction plateau age from sample 89GP71. This pattern may reflect partial argon loss in igneous muscovite that was subjected to grain-size reduction in the shear zones. However, given the intense fabric development in the shear zones, this interpretation seems unlikely, as the white mica appears to be new mineral growth. An alternative explanation of this release pattern is that the mica separate contained two distinct mica populations: (*i*) older mica similar to sample 89GP71, and (*ii*) new mica from within the shear zones that

Fig. 8. $^{40}Ar/^{40}Ar$ release spectra with plateau ages and errors for hornblende from sample 89SR29, biotite from sample 89GP61, and muscovite from samples 89GP71 and 90KS18. Analytical data are given in Table 5 for samples 89GP61 and 90KS18 and in Roeske et al. (1992) for samples 89SR29 and 89GP71. Sample locations are shown in Fig. 2.

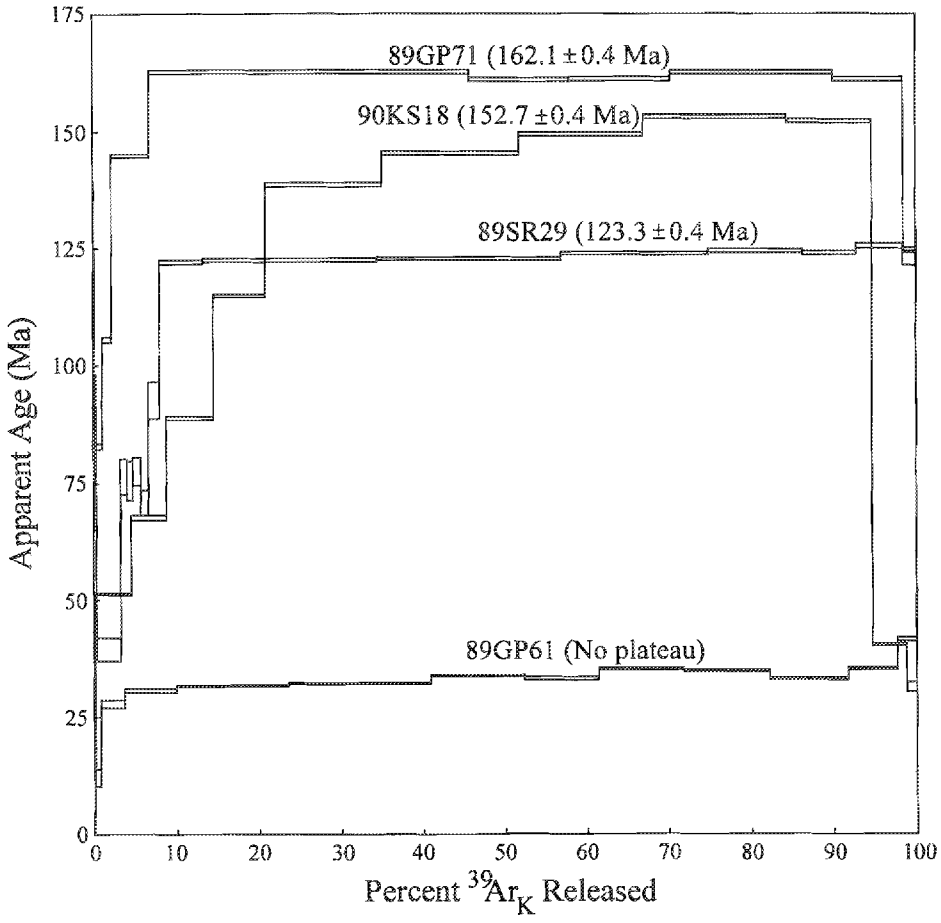

were much younger. Regardless of which interpretation is preferred, the low-temperature portion of the release spectrum implies that deformation and associated low-grade metamorphism were still active at ~50 Ma.

Depth estimate for the deformational events along the Border Ranges shear zone

The Lamplugh pluton (samples 90KS5 and 89GP5X, Fig. 2) along the eastern side of the BRSZ has the necessary assemblage for the Al-in-hornblende geobarometer (e.g., Hammarstrom and Zen 1986; Hollister et al. 1987). Table 5 presents representative mineral compositions analyzed at Rice University on a Cameca SX-50 electron microprobe using natural and synthetic oxide standards. X-ray intensities were converted to weight percent by the $\varphi(\rho z)$ algorithm of Pouchou and Pichoir (1991). Recently, others have proposed that this geobarometer be calibrated for temperature effects (Leake and Said 1994; Anderson and Smith 1995). Crystallization temperatures of ~715°C were estimated with the Holland and Blundy (1994) amphibole–plagioclase geothermometer. The calibrations of Schmidt (1992) and Anderson and Smith (1995) seem best suited for this pluton and yield crystallization pressures (Table 5) between 250 ± 60 and 350 ± 60 MPa. This provides a maximum depth for the deformation of approximately 10–12 km.

Discussion and conclusions

Movement history of the Border Ranges shear zone in Glacier Bay

Our kinematic analysis of the ductile shear zones and brittle faults within the BRSZ shows predominantly subhorizontal dextral motion. Micro- and mesoscale kinematic indicators demonstrate consistent dextral shear along steep to near-vertical surfaces with a nearly horizontal slip line. Mineral lineations, extension lineations calculated from S–C intersections, and slickenlines on brittle fault planes further document subhorizontal motion.

We propose that much, or all, of the low-temperature deformation recognized in the BRSZ occurred during the early Cenozoic, as sample 90KS18 (Fig. 8) has evidence for an early Cenozoic white mica population. This interpretation of the age spectrum supports our field interpretation that the phyllite–greywacke assemblages incorporated in the BRSZ represent the latest Cretaceous flysch unit of the Chugach terrane. The involvement of these rocks does not necessarily constrain the age of deformation because (*i*) lithologic corre-

Table 4. $^{40}Ar/^{39}Ar$ analytical data for samples 89GP61 and 90KS18 (locations given in Fig. 2).

Temp. (°C)	Radiogenic ^{40}Ar (V)	K-derived ^{39}Ar (V)	*F* value	Radiogenic yield (%)	Percent ^{39}Ar total	$^{39}Ar/^{37}Ar$ ratio	Apparent age and error (Ma at 1σ)
Sample 89GP61: biotite, latitude 58°54′18″N, longitude 137°01′18″W							
500	0.00192	0.00182	1.053	2.6	0.1	143.55	15.46±34.18
600	0.02106	0.02577	0.817	8.8	0.7	1.71	12.01±1.86
650	0.19533	0.10247	1.906	49.1	2.9	7.58	27.89±0.82
700	0.46849	0.22364	2.095	61.8	6.3	5.88	30.63±0.36
750	1.03325	0.47889	2.164	87.8	13.5	31.26	31.63±0.14
800	1.33789	0.61121	2.189	95.8	17.3	19.14	32.00±0.15
850	0.94376	0.40854	2.310	96.5	11.5	18.87	33.75±0.17
900	0.77773	0.32050	2.268	95.2	9.1	14.50	33.13±0.37
950	0.88185	0.36637	2.407	92.8	10.4	13.04	35.15±0.17
1000	0.87396	0.36836	2.373	93.1	10.4	13.90	34.66±0.18
1050	0.67976	0.30126	2.256	94.0	8.5	10.72	32.97±0.26
1150	0.51509	0.21333	2.415	92.0	6.0	1.00	35.26±0.20
1300	0.33109	0.11658	2.840	86.7	3.3	1.25	41.40±0.41
Total gas			2.264				33.09±0.30
Sample 90KS18: muscovite, latitude 58°54′12″N, longitude 136°59′30″W							
500	0.01149	0.00864	1.329	8.6	0.2	11.13	17.22±2.92
700	0.67805	0.16960	3.998	58.3	4.3	6.83	51.30±0.21
750	0.90027	0.17004	5.295	90.0	4.3	11.70	67.63±0.58
800	1.57589	0.22547	6.989	97.3	5.7	7.25	88.75±0.34
850	2.28180	0.25030	9.116	97.6	6.3	13.68	114.92±0.33
900	6.22159	0.56183	11.074	98.7	14.2	27.99	138.67±0.44
950	7.69609	0.66199	11.626	98.9	16.8	17.49	145.31±0.39
1000	7.16826	0.59929	11.961	98.7	15.2	16.87	149.33±0.40
1050	8.42662	0.68657	12.274	98.9	17.4	17.75	153.07±0.41
1160	4.97753	0.40837	12.189	98.8	10.3	10.30	152.06±0.40
1250	0.50663	0.16213	3.125	87.5	4.1	3.38	40.22±0.24
1350	0.10449	0.04304	2.428	79.1	1.1	7.51	31.22±1.04
Total gas			10.273				128.98±0.46

Notes: Analytical data for radiogenic ^{40}Ar and K-derived ^{39}Ar are calculated from raw data to five places right of the decimal; *F* values (radiogenic ^{40}Ar / K-derived ^{39}Ar after all corrections for interfering isotopes have been made) are calculated to three places right of the decimal. Radiogenic ^{40}Ar, K-derived ^{39}Ar, and *F* values have been rounded using calculated analytical precisions. Apparent ages and errors were calculated from unrounded data and then rounded using analytical precisions. $^{39}Ar/^{37}Ar$ is determined by mass spectrometry. Assuming ^{37}Ar is Ca derived and ^{39}Ar is K derived, this ratio is an "apparent K/Ca ratio" when multiplied by approximately 0.5.

lation is inherently ambiguous, as the metasedimentary rocks may not be from the latest Cretaceous flysch; and (*ii*) it is possible that the lithologic juxtaposition in the western half of the BRSZ is entirely the product of a brittle deformation that is distinctly younger than the development of the retrograde shear zones and fabrics. Nonetheless, when the observations are taken together, it seems more likely that the brittle and low-temperature ductile deformational history of the BRSZ are part of a progressive deformation event. The kinematics of the ductile and brittle deformational events are identical and many of the retrograde shear zones have very sharp boundaries. The lower greenschist to subgreenschist metamorphic assemblages indicate that the retrograde shear zones formed in the temperature range appropriate for the brittle–ductile transition.

This interpretation is potentially significant, because it may indicate that the low-temperature deformation along the BRSZ represents a progressive deformation at conditions near the brittle–ductile transition. This is indicated by the presence of synchronous ductile shear zones and brittle faults and their near parallelism. This observation could also be explained by superposition of structures. However, two observations support simultaneous brittle and ductile deformation: (*i*) most shear zone walls are sharp and the chloritic phyllonites within them are developed by recrystallization, and (*ii*) mineral assemblages in both faults and retrograde shear zones indicate a similar temperature for formation. This similarity may imply that a fluid-actuated process, such as initial brittle deformation, which allows fluid influx and alteration followed by a switch of deformation mechanism, was operational (e.g., Janecke and Evans 1988).

Our interpretation that dextral displacement was occurring at ~50 Ma is supported by other $^{40}Ar/^{39}Ar$ data along the Border Ranges fault system. Three hundred kilometres

Table 5. Representative mineral compositions and geothermobarometric estimates for two samples of the Early Cretaceous granodiorite (locations given in Fig. 2).

Sample No.:	90KS5[a]	90KS5	89GP5X[a]	89GP5X	89GP5X
Mineral:	Mg-hornblende	Plagioclase	Mg-hornblende	Plagioclase	K-feldspar
SiO_2 (wt.%)	47.74	58.63	45.42	63.10	63.24
TiO_2	0.91	na	1.32	na	na
Al_2O_3	7.34	25.88	8.39	23.08	18.70
FeO	15.21	0.52	16.64	0.52	0.25
MnO	0.51	na	0.50	na	na
MgO	13.07	na	11.66	na	na
CaO	11.83	7.13	11.84	2.22	0.04
Na_2O	1.06	7.14	1.10	9.06	0.49
K_2O	0.47	0.07	0.94	1.96	15.63
BaO	na	0.11	na	0.11	1.01
F	0.12	na	0.12	na	na
Cl	0.05	na	0.18	na	na
H_2O[b]	2.00	na	1.93	na	na
O = F + Cl	0.06	na	0.09	na	na
Total	100.84	99.49	100.46	100.05	99.38
No. of oxygens	23	8	23	8	8
Si	6.918	2.631	6.708	2.804	2.963
Al^{iv}	1.082	1.369	1.292	1.209	1.033
Al^{vi}	0.172	—	0.169	—	—
Ti	0.099	—	0.146	—	—
Fe^{3+}	0.656	0.018	0.593	0.017	0.009
Fe^{2+}	1.188	—	1.462	—	—
Mn	0.062	—	0.063	—	—
Mg	2.823	—	2.567	—	—
Ca	1.836	0.343	1.873	0.781	0.002
Na	0.298	0.622	0.314	0.781	0.045
K	0.087	0.004	0.177	0.111	0.935
Ba	—	0.002	—	0.002	0.019
F	0.055	—	0.056	—	—
Cl	0.013	—	0.044	—	—
Pressure (MPa)					
Hammarstrom and Zen (1986)	240		340		
Hollister et al. (1987)	230		350		
Johnson and Rutherford (1989)	180		270		
Schmidt (1992)	300		390		
Anderson and Smith (1995)	250		350		
Temperature (°C)[c]	719		713		

Notes: na, not analyzed.
[a]Amphibole stoichiometry calculated using Tindle and Webb (1994).
[b]H_2O is calculated by difference.
[c]Temperature is calculated using Holland and Blundy (1994).

to the northwest, Roeske et al. (1993) documented ductile deformation in a dextral strike-slip zone along the Border Ranges fault system between 58 and 51 Ma. Two hundred and twenty kilometres to the south, on Baranof Island, veins associated with brittle deformation on a dextral strike-slip fault in the Border Ranges fault system have a white mica $^{40}Ar/^{39}Ar$ date of 49.5 Ma (Haeussler et al. 1994, 1995). If the dextral slip recorded in the BRSZ of Glacier Bay occurred simultaneously with these Early Eocene displacements, then the active fault system was over 500 km in length.

Although the kinematics of the low-temperature deformation are clear, the older history of the BRSZ is not well resolved. Microstructures in the foliated plutonic rocks, together with the elongate shape of the pluton, suggest emplacement as a syntectonic intrusive. Estimated finite strains are consistent with the dominance of S-tectonites in the high-temperature fabric. Since flattening strains are predicted from theoretical models of transpressional systems (Fossen and Tikoff 1993), the syntectonic emplacement may have occurred within a transpressional shear zone. Further work is needed, but if this tentative conclusion is substantiated, then the BRSZ may have two distinct episodes of

transcurrent motion. The early history may be concurrent with the Early Cretaceous emplacement of the plutonic body and later dextral strike-slip movement.

Tectonic significance

The Border Ranges shear zone in northern Glacier Bay records ancient arc-parallel strike-slip similar to modern oblique convergent margins such as Sumatra, northern Chile, and the western Aleutians (Fitch 1972; Jarrard 1986; Scheuber and Andriessen 1990; Diament et al. 1992; McCaffrey 1992). The main strike-slip event recorded by the low-temperature fabrics and faults in this system was apparently of Paleocene or Early Eocene age. The timing of this event is important, because early Cenozoic dextral strike-slip is widespread in the northern Cordillera, and this motion has generally been attributed to the effects of oblique subduction of the Kula plate (e.g., Plafker et al. 1994). Moreover, the presence of a major dextral fault along the inboard edge of the Chugach terrane may resolve a long-standing problem posed by paleomagnetic data (Plumley et al. 1983; Bol et al. 1992), which indicate greater Tertiary poleward displacement in the Chugach terrane than in the more inboard Peninsular and Wrangellia terranes. No piercing points exist that might resolve the net dextral slip on the BRSZ in Glacier Bay, but even the minimum offset from the paleomagnetic data indicates displacements greater than 400 km (Bol et al. 1992).

Hints of the magnitude of the net slip on the BRSZ were suggested by Roeske et al. (1992), who noted that the 162 Ma cooling ages for plutonic rocks within the zone were atypical of the Glacier Bay area. The closest plutons along strike from Glacier Bay with similar cooling ages are ~150 km to the south, on Chichagof Island (Brew and Morrell 1983; Karl et al. 1988). This apparent displacement would be a minimum, as plutons of that age range occur in the Queen Charlotte Islands and Vancouver Island, 600–800 km to the south (Anderson and Greig 1989; Anderson and Reichenbach 1989; Friedman 1990). Similarly, the ~130 Ma age for the foliated pluton along the BRSZ in Glacier Bay is an unusual date in the northern Cordillera. Rare cooling ages as young as ~130 Ma have been reported to the northwest in the St. Elias Range (Dodds and Campbell 1988; Campbell and Dodds 1991; Woodsworth et al. 1991). The next youngest suite of plutonic rocks, the Nutzotin–Chichagof belt of Hudson (1979, 1983), encompasses cooling dates of 117–100 Ma. The ~130 Ma pluton in Johns Hopkins Inlet may be part of this suite, but if so it would be the oldest date reported from it. Intrusive rocks of similar age (120–130 Ma) do occur, however, 700 km along strike in the western Chugach Mountains (Pavlis et al. 1988; Barnett et al. 1994). It is possible that these two plutonic complexes are part of an original plutonic complex that has now been dispersed by strike-slip. If this speculation is correct, the net slip on the Border Ranges fault system may be comparable to, or larger than, other well-known dextral structures like the Denali and Tintina faults.

The significance of the early deformation indicated by the syntectonic emplacement fabrics of the ~130 Ma pluton along the BRSZ is still poorly resolved. The apparent age of the event represents a time when major thrusting was occurring along segments of the Border Ranges fault system now located in the western Chugach Mountains (Pavlis et al. 1988; Barnett et al. 1994). Thus, the syntectonic emplacement of the pluton in Glacier Bay could record a related event. However, this association is cryptic, and until more information is available on the pre-Cenozoic history of the Glacier Bay region, this question will remain unresolved.

Acknowledgments

This project was supported by Louisiana Educational Trust Fund Grant LEQSF-RD-A-25 and National Science Foundation grant EAR-9105199 (to Pavlis), National Science Foundation grant EAR-9105499 (to Roeske), and National Science Foundation grant EAR-9304062 (to Sisson). Invaluable logistical support was provided by Marc Schroeder, Greg Streveler, and all the park service personnel in Glacier Bay National Park and Preserve, and Dr. David Brew is thanked for the use of some of his field equipment. This manuscript benefited greatly from thorough and critical reviews by David J.W. Piper, Randall R. Parrish, George E. Gehrels, David A. Brew, and William M. Dunne. This work represents part of K.J. Smart's M.S. thesis at the University of New Orleans.

References

Anderson, J.L., and Smith, D.R. 1995. The effects of temperature and f_{O_2} on the Al-in-hornblende barometer. American Mineralogist, 80: 549–559.

Anderson, R.G., and Greig, C.J. 1989. Jurassic and Tertiary plutonism in the Queen Charlotte Islands, British Columbia. *In* Current Research, part H. Geological Survey of Canada, Paper 89-1H, pp. 95–104.

Anderson, R.G., and Reichenbach, I. 1989. A note on the geochronometry of Late Jurassic and Tertiary plutonism in the Queen Charlotte Islands, British Columbia. *In* Current research, part H. Geological Survey of Canada, Paper 89-1H, pp. 105–112.

Barnett, D.E., Bowman, J.R., Pavlis, T.L., Rubenstone, J.R., Snee, L.W., and Onstott, T.C. 1994. Metamorphism and near-trench plutonism during initial accretion of the Cretaceous Alaskan forearc. Journal of Geophysical Research, 99: 24 007 – 24 024.

Bol, A.J., Coe, R.S., Gromme, C.S., and Hillhouse, J.W. 1992. Paleomagnetism of the Resurrection Peninsula, Alaska: implications for the tectonics of southern Alaska and the Kula-Farallon Ridge. Journal of Geophysical Research, 97: 17 213 – 17 232.

Brew, D.A. 1994. Latest Mesozoic and Cenozoic magmatism, southeastern Alaska. *In* The geology of Alaska. *Edited by* G. Plafker and H.C. Berg. Geological Society of America, The Geology of North America, Vol. G-1, pp. 621–656.

Brew, D.A., and Morrell, R.P. 1978. Tarr Inlet suture zone, Glacier Bay National Monument, Alaska. United States Geological Survey, Circular 772-B, pp. B90–B92.

Brew, D.A., and Morrell, R.P. 1979*a*. The Wrangell terrane ("Wrangellia") in southeastern Alaska: the Tarr Inlet suture zone with its northern and southern extensions. United States Geological Survey, Circular 804-B, pp. B121–B123.

Brew, D.A., and Morrell, R.P. 1979*b*. Intrusive rock belts of southeastern Alaska. United States Geological Survey, Circular 804-B, pp. B116–B121.

Brew, D.A., and Morrell, R.P. 1979*c*. Correlation of the Sitka Graywacke, unnamed rocks in the Fairweather Range, and Valdez Group, southeastern and south-central Alaska. United States Geological Survey, Circular 804-B, pp. B123–B125.

Brew, D.A., and Morrell, R.P. 1983. Intrusive rocks and plutonic belts of southeastern Alaska. *In* Circum-Pacific plutonic terranes. *Edited by* J.A. Roddick. Geological Society of America, Memoir 159, pp. 171–193.

Brew, D.A., Johnson, B.R., Ford, A.B., and Morrell, R.P. 1978*a*. Intrusive rocks in the Fairweather Range, Glacier Bay National

Monument, Alaska. United States Geological Survey, Circular 772-B, pp. B88–B90.

Brew, D.A., Johnson, B.R., Grybeck, D., Griscom, A., Barnes, D.F., Kimball, A.L., Still, J.C., and Rataj, J.L. 1978*b*. Mineral resources of the Glacier Bay National Monument wilderness study area, Alaska. United States Geological Survey, Open-file Report 78-494.

Brun, J.P., Gapais, D., Cogne, J.P., Ledru, P., and Vigneresse, J.L. 1990. The Flamanville granite (northwest France): an unequivocal example of a syntectonically expanding pluton. Geological Journal, **25**: 271–286.

Campbell, R.B., and Dodds, C.J. 1991. Saint Elias Mountains. *In* Geology of the Cordilleran Orogen in Canada. *Edited by* H. Gabrielse and C.J. Yorath. Geological Society of America, The Geology of North America, Vol. G-2, pp. 574–577.

Castro, A. 1987. On granitoid emplacement and related structures: a review. Geologische Rundschau, **76**: 101–124.

Coney, P.J., Jones, D.L., and Monger, J.W.H. 1980. Cordilleran suspect terranes. Nature (London), **288**: 329–333.

Debiche, M.G., Cox, A., and Engebretson, D. 1987. The motion of allochthonous terranes across the North Pacific Basin. Geological Society of America, Special Paper 207.

Decker, J.E., and Plafker, G. 1982. Correlation of the rocks in the Tarr Inlet suture zone with the Kelp Bay Group. United States Geological Survey, Circular 844, pp. 119–123.

Diament, M., Harjono, H., Karta, K., Deplus, C., Dahrin, D., Zen, M.T., Jr., Gerard, M., Lassal, O., Martin, A., and Malod, J. 1992. Mentawi fault zone off Sumatra: a new key to the geodynamics of western Indonesia. Geology, **20**: 259–262.

Dodds, C.J., and Campbell, R.B. 1988. K–Ar ages of mainly intrusive rocks in the Saint Elias Mountains, Yukon and British Columbia. Geological Survey of Canada, Paper 87-16.

Engebretson, D.C., Cox, A., and Gorden, R.C. 1985. Relative motions between oceanic and continental plates in the Pacific basin. Geological Society of America, Special Paper 206.

Engebretson, D.C., Cox, A., and Debiche, M. 1987. Reconstructions, plate interactions, and trajectories of oceanic and continental plates in the Pacific basin. *In* Circum-Pacific orogenic belts and evolution of the Pacific Ocean Basin. *Edited by* J.W.H. Monger and J. Francheteau. American Geophysical Union, Geodynamics Series, Vol. 18, pp. 19–27.

Erslev, E.A. 1988. Normalized center-to-center strain analysis of packed aggregates. Journal of Structural Geology, **10**: 201–209.

Fitch, T.J. 1972. Plate convergence, transcurrent faults and internal deformation adjacent to southeast Asia and the western Pacific. Journal of Geophysical Research, **77**: 4432–4460.

Fossen, H., and Tikoff, B. 1993. The deformation matrix for simultaneous simple shearing, pure shearing and volume change, and its application to transpression–transtension tectonics. Journal of Structural Geology, **15**: 413–422.

Friedman, R.M. 1990. U–Pb dating of Jurassic, Cretaceous, and Tertiary igneous rocks from the southern coast belt (49°–51°N), southwestern British Columbia. Geological Association of Canada – Mineralogical Association of Canada, Program with Abstracts, **15**: A41.

Gehrels, G.E., and Berg, H.C. 1994. Geology of southeastern Alaska. *In* The geology of Alaska. *Edited by* G. Plafker and H.C. Berg. Geological Society of America, The Geology of North America, Vol. G-1, pp. 451–467.

Haeussler, P.J., Davis, J.S., and Roeske, S.M. 1994. Late Mesozoic and Cenozoic faulting at the leading edge of North America, Chichagof and Baranof Islands, southeastern Alaska. Geological Society of America, Abstracts with Programs, **26**: A317.

Haeussler, P.J., Bradley, D., Goldfarb, R., Snee, L., and Taylor, C. 1995. Link between ridge subduction and gold mineralization in southern Alaska. Geology, **23**: 995–998.

Hammarstrom, J.M., and Zen, E.-A. 1986. Aluminum in hornblende: an empirical igneous geobarometer. American Mineralogist, **71**: 1297–1313.

Holland, T., and Blundy, J. 1994. Non-ideal interactions in calcic amphiboles and their bearing on amphibole–plagioclase thermometry. Contributions to Mineralogy and Petrology, **116**: 433–447.

Hollister, L.S., Grissom, G.C., Peters, E.K., Stowell, H.H., and Sisson, V.B. 1987. Confirmation of the empirical correlation of Al in hornblende with pressure of solidification of calc-alkaline plutons. American Mineralogist, **72**: 231–239.

Hudson, T. 1979. Mesozoic plutonic belts of southern Alaska. Geology, **7**: 230–234.

Hudson, T. 1983. Calc-alkaline plutonism along the Pacific rim of southern Alaska. *In* Circum-Pacific plutonic terranes. *Edited by* J.A. Roddick. Geological Society of America, Memoir 159, pp. 159–169.

Hutton, D.H.W. 1988. Granite emplacement mechanisms and tectonic controls: inferences from deformation studies. Transactions of the Royal Society of Edinburgh: Earth Sciences, **79**: 245–255.

Janecke, S.U., and Evans, J.P. 1988. Feldspar-induced rock rheologies. Geology, **16**: 1064–1067.

Jarrard, R.D. 1986. Terrane motion by strike-slip faulting of forearc slivers. Geology, **14**: 780–783.

Johnson, M.C., and Rutherford, M.J. 1989. Experimental calibration of the aluminum-in-hornblende geobarometer with application to Long Valley caldera (California) volcanic rocks. Geology, **17**: 837–841.

Jones, D.L., Silberling, N.J., Berg, H.C., and Plafker, G. 1981. Tectonostratigraphic terrane map of Alaska. United States Geological Survey, Open-file Report 81-792.

Kamb, W.B. 1959. Ice petrofabric observations from Blue Glacier, Washington, in relation to theory and experiment. Journal of Geophysical Research, **64**: 1891–1909.

Karl, S.M., Johnson, B.R., and Lanphere, M.A. 1988. New K–Ar ages from plutons on western Chichagof Island and on Yakobi Island. *In* Geologic studies in Alaska by the U.S. Geological Survey during 1987. *Edited by* J.P. Galloway and T.D. Hamilton. United States Geological Survey, Circular 1016, pp. 164–168.

Leake, B.E., and Said, Y.A. 1994. Hornblende barometry of the Galway batholith, Ireland: an empirical test. Mineralogy and Petrology, **51**: 243–250.

MacKevett, E.M., and Plafker, G. 1974. The Border Ranges fault in south-central Alaska. Journal of Research of the United States Geological Survey, **2**: 323–329.

McCaffrey, R. 1992. Oblique plate convergence, slip vectors, and forearc deformation. Journal of Geophysical Research, **97**: 8905–8915.

McDougall, I., and Harrison, T.M. 1988. Geochronology and thermochronology by the $^{40}Ar/^{39}Ar$ method. Oxford Monographs on Geology and Geophysics, No. 9. Oxford University Press, New York.

Miller, R.B., and Paterson, S.R. 1992. Tectonic implications of syn- and post-emplacement deformation of the Mount Stuart batholith for mid-Cretaceous orogenesis in the North Cascades. Canadian Journal of Earth Sciences, **29**: 479–485.

Oldow, J.S., Bally, A.W., Avé Lallemant, H.G., and Leeman, W.P. 1989. Phanerozoic evolution of the North American Cordillera: United States and Canada. *In* The geology of North America — an overview. *Edited by* A.W. Bally and A.R. Palmer. Geological Society of America, The Geology of North America, Vol. A, pp. 139–232.

Owens, W.H. 1984. The calculation of a best-fit ellipsoid from elliptical sections on arbitrarily oriented planes. Journal of Structural Geology, **6**: 571–578.

Panozzo, R. 1983. Two-dimensional analysis of shape fabric using projections of digitized lines in a plane. Tectonophysics, **95**: 279–294.

Panozzo, R. 1984. Two-dimensional strain from the orientation of lines in a plane. Journal of Structural Geology, **6**: 215–221.

Paterson, S.R., and Fowler, T.K. 1993. Re-examining pluton emplacement processes. Journal of Structural Geology, **15**: 191–206.

Paterson, S.R., Vernon, R.H., and Tobisch, O.T. 1989. A review of criteria for the identification of magmatic and tectonic foliations in granitoids. Journal of Structural Geology, **11**: 349–363.

Pavlis, T.L. 1982. Origin and age of the Border Ranges fault of southern Alaska and its bearing on the late Mesozoic tectonic evolution of Alaska. Tectonics, **1**: 343–368.

Pavlis, T.L., and Crouse, G.W. 1989. Late Mesozoic strike-slip movement on the Border Ranges fault system in the eastern Chugach Mountains, southern Alaska. Journal of Geophysical Research, **94**: 4321–4332.

Pavlis, T.L., Monteverde, D.H., Bowman, J.R., Rubenstone, J.L., and Reason, M.D. 1988. Early Cretaceous near-trench plutonism in southern Alaska: a tonalite–trondhjemite intrusive complex injected during ductile thrusting along the Border Ranges Fault System. Tectonics, **7**: 1179–1199.

Pavlis, T.L., Roeske, S.M., Sisson, V.B., and Smart, K.J. 1989. Evidence for Cretaceous dextral strike-slip on the Border Ranges Fault in Glacier Bay National Park, Alaska. Eos, **70**: 1337.

Plafker, G. 1987. Regional geology and petroleum potential of the northern Gulf of Alaska continental margin. *In* Geology and resource potential of the continental margin of western North America and adjacent ocean basins. *Edited by* D.W. Scholl, A. Grantz, and J.G. Vedder. Circum-Pacific Council for Energy and Mineral Resources, Earth Science Series, Vol. 6, pp. 229–268.

Plafker, G., Jones, D.L., and Pessagno, E.A., Jr. 1977. A Cretaceous accretionary flysch and melange terrane along the Gulf of Alaska margin. *In* The United States Geological Survey in Alaska: accomplishments during 1976. *Edited by* K.M. Blean. United States Geological Survey, Circular 751-B, pp. B41–B43.

Plafker, G., Nokleberg, W.J., and Lull, J.S. 1989. Bedrock geology and tectonic evolution of the Wrangellia, Peninsular, and Chugach terranes along the Trans-Alaska Crustal Transect in the Chugach Mountains and southern Copper River basin, Alaska. Journal of Geophysical Research, **94**: 4255–4295.

Plafker, G., Moore, J.C., and Winkler, G.R. 1994. Geology of the southern Alaska margin. *In* The geology of Alaska. *Edited by* G. Plafker and H.C. Berg. Geological Society of America, The Geology of North America, Vol. G-1, pp. 389–449.

Plumley, P.W., Coe, R.S., and Byrne, T. 1983. Paleomagnetism of the Paleocene Ghost Rocks formation, Prince William terrane, Alaska. Tectonics, **2**: 295–314.

Pouchou, J.L., and Pichoir, F. 1991. Quantitative analysis of homogeneous or stratified microvolumes applying the "PAP". *In* Electron microprobe quantification. *Edited by* K.F.J. Heinrich and D.E. Newbury. Plenum, New York, pp. 31–75.

Ramsay, J.G. 1989. Emplacement kinematics of a granite diapir: the Chindamora batholith, Zimbabwe. Journal of Structural Geology, **11**: 191–209.

Ramsay, J.G., and Huber, M.I. 1983. The techniques of modern structural geology. Vol. 1: strain analysis. Academic Press, London.

Roeske, S.M., Mattinson, J.M., and Armstrong, R.L. 1989. Isotopic ages of glaucophane schists on the Kodiak Islands, southern Alaska, and their implications for the Mesozoic tectonic history of the Border Ranges fault system. Geological Society of America Bulletin, **101**: 1021–1037.

Roeske, S.M., Pavlis, T.L., Sisson, V.B., and Smart, K.J. 1990. Cretaceous strike-slip along the Border Ranges Fault System in eastern and southeastern Alaska. Geological Association of Canada – Mineralogical Association of Canada, Program with Abstracts, **15**: A113.

Roeske, S.M., Snee, L.W., and Pavlis, T.L. 1991. Strike-slip and accretion events along the southern Alaska plate margin in the Cretaceous and early Tertiary. Geological Society of America, Abstracts with Programs, **23**: A428.

Roeske, S.M., Pavlis, T.L., Snee, L., and Sisson, V.B. 1992. $^{40}Ar/^{39}Ar$ isotopic ages from the Wrangellia–Alexander Terrane along the Border Ranges Fault System in the eastern Chugach Mountains and Glacier Bay, Alaska. *In* Geologic studies in Alaska by the United States Geological Survey, 1990. United States Geological Survey, Bulletin 1999, pp. 180–195.

Roeske, S.M., Snee, L.W., and Bunds, M.P. 1993. $^{40}Ar/^{39}Ar$ dates from the Border Ranges fault system, a hydrothermally altered brittle–ductile transition strike-slip shear zone, southern Alaska. Geological Society of America, Abstracts with Programs, **25**: A419.

Sanderson, D.J., and Marchini, W.R.D. 1984. Transpression. Journal of Structural Geology, **6**: 449–458.

Scheuber, E., and Andriessen, P.A.M. 1990. The kinematic and geodynamic significance of the Atacama fault zone, northern Chile. Journal of Structural Geology, **12**: 243–257.

Schmidt, M.W. 1992. Amphibole composition in tonalite as a function of pressure: an experimental calibration of the Al-in-hornblende barometer. Contributions to Mineralogy and Petrology, **110**: 304–310.

Tindle, A.G., and Webb, P.C. 1994. PROBE-AMPH — a spreadsheet program to classify microprobe-derived amphibole analyses. Computers and Geoscience, **20**: 1201–1228.

Woodsworth, G.J., Anderson, R.G., and Armstrong, R.L. 1991. Plutonic regimes. *In* Geology of the Cordilleran Orogen in Canada. *Edited by* H. Gabrielse and C.J. Yorath. Geological Society of America, The Geology of North America, Vol. G-2, pp. 491–531.